

# Brightness induction from rods

Hao Sun<sup>1</sup>

Visual Sciences Center, University of Chicago, Chicago, IL, USA



Joel Pokorny

Visual Sciences Center, University of Chicago, Chicago, IL, USA



Vivianne C. Smith

Visual Sciences Center, University of Chicago, Chicago, IL, USA



<sup>1</sup>Current address:

State University of New York, College of Optometry, New York, NY, USA

Rod modulation of an annular surround can produce brightness contrast in a test field centered at 10° from the fovea. In our research, stimuli originated from a colorimeter that provided 4 primaries in both the circular test and the annular surround fields, and allowed independent modulation of the rods and each of the short (S)-, middle (M)-, and long (L)-wavelength-sensitive cone types. The chromaticity was set so fields had the same appearance as the equal energy spectrum. At 1 photopic troland (td), rod-induced modulation in the test field could be cancelled by either a rod- or a cone-nulling modulation added to the test field. The best cone nulling of rod induction showed residual flicker. Nulling was more effective, though still imperfect, with a cone-nulling stimulus of higher S-cone modulation contrast. Rod induction with square-wave, on-pulse, and off-pulse temporal profiles was closely similar. At higher light levels, 10 and 100 td, rod contrast could not be nulled by rod or cone modulation. The failure to achieve nulls may have been caused by either or both of the following hypotheses: (1) there is a mismatch between the rod and cone temporal waveforms; (2) there is strong rod input to the magnocellular pathway, but negligible rod input to the parvocellular pathway, as shown by single-unit electrophysiological data.

Keywords: rod, induction, brightness contrast, magnocellular, parvocellular

## Introduction

The color and brightness of an illuminated object does not depend solely on the physical light reflected from its surface. The appearance of the object depends also on the chroma and luminance of an adjacent or nearby field. One well-known induction effect is contrast. For brightness contrast, a test field appears darker when viewed in a more luminous surround. There are many contrast studies involving both color and brightness induction; see reviews of Wyszecki (1986) and Beck (1972). Brightness induction at photopic levels shows asymmetry between incremental and decremental induction (Heinemann, 1955). A bright surround induces disproportionately more darkness than a dark surround induces brightness.

Few studies have analyzed the potential contribution of rod stimulation to induction. Studies on scotopic induction have examined the perceived hue of a rod-test stimulus with either successively or simultaneously presented cone-inducing stimuli (Buck, 1997; Buck & Brandt, 1995; Stabell & Stabell, 1975; 1978). We are

not aware of studies that have evaluated changes in visual perception caused by rod-inducing stimuli.

We investigated rod induction with a new approach, using a 4 primary colorimetric system that allowed independent stimulation of all 4 types of photoreceptors in color normal trichromatic observers (Sun, Pokorny, & Smith, 2001a). The apparatus displayed a 6° circular central test in a 16° annular surround. A fixation target placed the center of the field at an eccentricity of 10° in the temporal retina. The retinal region subtended by the central field, between 7° and 13°, is anatomically homogeneous; there is little variation in receptor populations (Curcio, Sloan, Kalina, & Hendrickson, 1990), photoreceptor dimensions (Hendrickson & Drucker, 1992), or macular pigment density (Hammond, Wooten, & Snodderly, 1997; Moreland & Bhatt, 1984).

By using a modulation technique with a nulling task (Krauskopf, Zaidi, & Mandler, 1986; Zaidi, Yoshimi, & Flannigan, 1991), we could investigate the effect of a rod- or cone-inducing stimulus in the annular surround. The amount of induction could be assessed for either a rod- or cone-nulling test. To look for asymmetry in incremental and decremental contrast surrounds, we

used asymmetric incremental and decremental modulation. We found that modulation of rod activity in an annular surround altered the appearance of the center. The center modulation could be nulled by rod or cone modulation of the test field at low (1 troland [td]) but not at higher (10-100 td) retinal illuminances.

## Methods

### Apparatus

A Macintosh Quadra 950 computer and 4 National Instruments (Austin, TX) interface boards (MIO-16, AO-6, and 2 DMA 2800) controlled an 8-channel colorimeter (Figure 1).

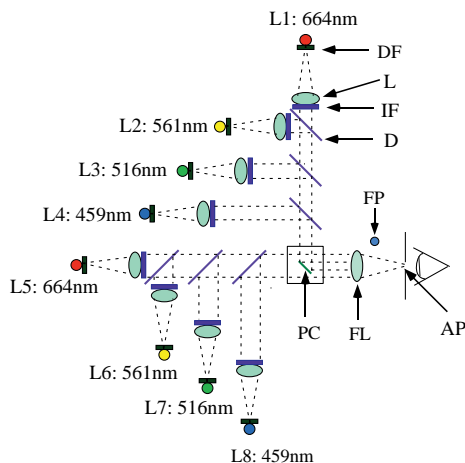


Figure 1. Eight-channel colorimeter diagram. L1 to L4 are center light-emitting diodes (LEDs); L5 to L8 are surround LEDs. Light from each LED passed through plastic diffusers (DF) before being collimated by a lens (L), and passing through an interference filter (IF). The LED/filter combinations produced primaries with dominant wavelengths of 459, 516, 561, and 664 nm. Lights within the center and the surround pathways were combined using dichroic mirrors (D). A photometric cube (PC) with a mirrored ellipse on the hypotenuse formed the center-surround field configuration. A field lens (FL) focused the LED images on the 2-mm artificial pupil (AP), and produced an image of the field at optical infinity.

The colorimeter presented a  $6^\circ$  circular center and a  $16^\circ$  annular surround. The center and surround each consisted of 4 channels. The optics of the center and surround channels were identical prior to combination. Light from each light-emitting diode (LED) (L1-L8) was first spatially homogenized by 2 spaced holographic diffusers (Physical Optics, Torrance, CA;  $20^\circ$  angle of diffusion), and then collimated by a lens (76-mm focal

length; 29-mm diameter). Collimated light from each LED passed through a 3-cavity interference filter. The 4 lights within the center or surround pathway were merged using dichroic mirrors, then focused on a 2-mm artificial pupil by a field lens (60-mm focal length; 29-mm diameter). The center-surround field configuration was formed by a photometric cube with a mirrored ellipse on the hypotenuse. The photometric cube was placed 1 focal length away from the field lens; hence, the image of the center-surround field was focused at optical infinity. The optical pathlengths from each of the 8 LEDs to the field lens were identical. The head of the observer was held stable by a chin-rest, with the superciliary ridge of the viewing eye resting against the eyepiece. Each observer's eye was 8 mm from the artificial pupil. The size of the surround LED beam at this location, measured with an optical comparator, was 2.2 mm in diameter. This size is consistent with the calculated beam half-height width. A fixation point allowed the field to be viewed at  $10^\circ$  in the temporal retina. Inconel neutral density filters, calibrated for each primary, were inserted in the final common path to control the average light level. The LED/interference filter combinations determined the spectra of the primaries. The peak wavelengths of the 4 primaries for both center and surround were 459, 516, 561, and 664 nm with half-height bandwidths of 8-10 nm. LEDtronics (Torrance, CA) manufactured the LEDs for the 459- and 664-nm primaries; the 516- and 561-nm primaries originated from Nichia LEDs (San Jose, CA). The LED luminance output was controlled by a train of 2 microsec constant-amplitude pulses with varying density provided by the LED drivers. Twelve-bit digital/analog (D/A) converters fed the LED drivers. A potentiometer scaled the input voltage to the LED driver and, therefore, allowed adjustment of the maximum luminance output of each LED. To maximize the bit resolution of the primaries, gelatin neutral density filters were added to 459-nm (0.9 log unit), 516-nm (0.6 log unit), and 664-nm (0.3 log unit) primaries, so that the DA output voltage for each LED was near 50% of its maximum for a stimulus of illuminance 100 photopic td and a chromaticity metameric to the equal energy spectrum.

### Calibration

The spectral distributions and the radiant outputs of the primaries were measured at the eyepiece. The spectral output of each channel was measured at the maximum LED output with an Optronics (Orlando, FL) OL754 spectroradiometer at 2-nm intervals. Although

the pulse-frequency modulation technique offers high LED output linearity over a 3-log unit range for modulation around a mean level (Swanson, Ueno, Smith, & Pokorny, 1987), we observed small but systematic deviations from linearity with variation in steady light level. These deviations are presumably caused by thermal effects associated with changes of current in the diode junction (Watanabe, Mori, & Nakamura, 1992).

Linearization of each LED output was attained with 3 linear equations for the ranges of 0.1-1, 0.01-0.1, and 0.001-0.01 of the maximum LED output. The maximum photopic illuminance output of the center 561-nm LED was measured with an EG&G (Gaithersburg, MD) 550 radiometer/photometer and used as a reference to calculate the illuminances of other LEDs.

## Observers

Two observers, H.S. (author) and S.S. (naïve to the purpose and design of the experiments), were normal trichromats as assessed with Ishihara pseudoisochromatic plates and the Neitz OT anomaloscope. H.S. had a Farnsworth-Munsell 100-hue error score of 4, and S.S. had an error score of 20. H.S. was myopic (-5.5) and wore nontinted contact lenses during the experiment. S.S. was emmetropic.

## Use of a 4 Primary Colorimetric System

Shapiro, Pokorny, and Smith (1996) gave a theoretical introduction to a 4 primary colorimetric system. To implement a 4 primary colorimetric system, it is necessary to have accurate estimates of an individual observer's receptor spectral sensitivities and prereceptoral filtering. First, we developed a technique to evaluate whether an individual observer's receptor sensitivities could be characterized as linear transforms of standard observer data after correcting for prereceptoral filtering differences between the individual and the standard observer.

The CIE scotopic luminosity function  $V'(\lambda)$  can be decomposed into 2 components: the spectral sensitivity of the photoreceptor at the retina, and the spectral transmittance of the prereceptoral filters:

$$V'(\lambda) = W'(\lambda) F_s(\lambda) \quad (1)$$

where  $W'(\lambda)$  represents the CIE  $V'(\lambda)$  expressed at the retinal level and  $F_s(\lambda)$  represents transmittance of the prereceptoral filter associated with the standard observer for scotopic photometry. The physiological basis of the  $W'(\lambda)$  distribution is the rhodopsin-absorption spectrum. We assume  $W'(\lambda)$  is invariant across observers because no rhodopsin polymorphisms have been reported for

human observers with normal visual function (Sung et al, 1991). Prereceptoral filter transmittances  $F(\lambda)$  are known to vary among observers. For a scotopic luminance match between 2 narrow band lights, reference light  $P_{ref}$  and a test light  $P_{test}$ , the standard observer match is given by

$$\int P_{test}(\lambda) W'(\lambda) F_s(\lambda) d\lambda = a_s \int P_{ref}(\lambda) W'(\lambda) F_s(\lambda) d\lambda \quad (2)$$

where  $a_s$  is calculated based on  $V'(\lambda)$ . For a scotopic match made by an individual observer

$$\int P_{test}(\lambda) W'(\lambda) F_o(\lambda) d\lambda = a_o \int P_{ref}(\lambda) W'(\lambda) F_o(\lambda) d\lambda \quad (3)$$

where  $F_o(\lambda)$  is the prereceptoral filter transmittance for the individual observer, and  $a_o$  is set by the individual observer. Ratio  $a_s/a_o$  represents the ratio of the prereceptoral filtering for the standard observer and an individual observer. Scotopic-luminance matching can be used to assess the prereceptoral difference between an individual observer and the standard observer for wavelengths where the scotopic sensitivity is higher than the photopic sensitivity. In particular, this method is appropriate for primaries 459, 516, and 561 nm.

At long wavelengths, the cones and the rods have similar sensitivities, preventing the use of a scotopic luminance match to calibrate individual prereceptoral filtering of the 664-nm primary. For this primary, we used a photopic colorimetric match. The CIE 10° standard observer for colorimetry has a unique match for the mixture of 459 and 561 nm matched to the mixture of 516 and 664 nm (Figure 2):

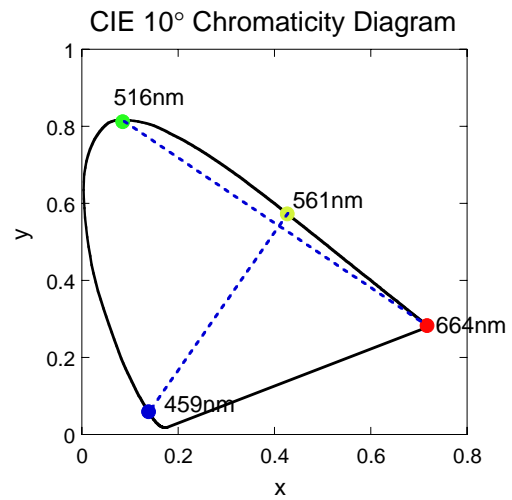


Figure 2. The equation (4) color match represented on the CIE 10° chromaticity diagram. The radiance of the 664-nm primary was adjustable; the radiances of the 459, 516, and 561 were set at the expected match for the CIE 10° standard observer, after correction for the differences in prereceptoral filtering between the individual and the standard observer.

$$b_1 459 \text{ nm} + 561 \text{ nm} = b_2 516 \text{ nm} + b_3 664 \text{ nm} \quad (4)$$

where  $b_1$ ,  $b_2$ , and  $b_3$  are the tristimulus values calculated from CIE 10° color-matching functions. For an individual observer, the values of the 459-, 516-, and 561-nm primaries are first corrected for the individual prereceptoral filtering differences measured by the scotopic luminance matches, and then they are fixed at the matching values  $b_1$ ,  $b_2$ , and 1.0. If the observer can make a color match by adjusting only the radiance of the 664-nm primary ( $b_3$ ), his or her receptoral spectral sensitivities at the 4 primary wavelengths can be approximated by linear transforms of the standard observer data. The difference between the 664-nm setting for the individual observer and the standard observer corrects for the individual prereceptoral transmittance at 664 nm.

### Heterochromatic Modulation Photometry

It is necessary to have accurate scotopic retinal illuminance matches to ensure good isolation of the rod and cone receptors. Heterochromatic modulation photometry (HMP) is a precise method for obtaining equiluminance for a pair of heterochromatic standard/test lights presented in temporal alternation (Pokorny, Smith, & Lutze, 1989). The average illuminance of the standard light is fixed, and the average illuminance of the test light is set at a series of prechosen values. On a given trial, the contrasts of the standard and test lights are adjusted in tandem to determine the contrast threshold. The contrast sensitivity, plotted as a function of the average illuminance of the test light, appears V shaped. If we fit the data with a V-shaped template, the equiluminant point between the test and standard lights can be estimated from the lowest sensitivity point of the template.

The HMP and color-matching experiments were performed separately for the 6° center or 16° annular surround. For the HMP measurements, the stimulus consisted of 2 primaries, a standard 561-nm primary, and a test primary that was either 459 or 516 nm. The standard and test primaries were square-wave modulated in counterphase at 6 Hz. The time-average illuminance of the standard primary was fixed at 0.08 photopic td, corresponding to 0.07 scotopic td. The time-average illuminance of the test primary varied from 0.04 scotopic td to 0.14 scotopic td. Four sets of HMP curves were obtained: center 561 and 459 nm, center 561 and 516 nm, surround 561 and 459 nm, and surround 561 and 516 nm. The method of adjustment was used to

obtain the modulation thresholds. The observer dark-adapted for 30 minutes prior to testing. Test illuminance was randomized from trial to trial in each session. Modulation thresholds and standard deviations were calculated from 10 threshold settings.

Each HMP data set was fitted with 2 templates (Pokorny et al, 1989), an illuminance-independent contrast template and an illuminance-dependent amplitude template. For a pair of temporally alternated standard and test lights, the psychophysical response amplitude,  $A$ , can be calculated as:

contrast template,

$$A = C / M_t \quad (5)$$

or amplitude template,

$$A = LC / L_0 M_t \quad (6)$$

where  $L$  is the time-average illuminance,  $C$  is the illuminance contrast of a pair of temporally alternated standard and test lights,  $L_0$  is a normalizing constant, and  $M_t$  is the optimal modulation threshold for human observer determined by the Weber fraction. The contrast template is appropriate if the time-average illuminance is constant, or if the temporal sensitivity is independent of illuminance level (Weber's law). The amplitude template is appropriate if the time-average illuminance is varied, or if the temporal sensitivity is dependent on illuminance level. The assumption that temporal sensitivity is independent of illuminance level is true at lower temporal frequencies, but not at higher temporal frequencies where the threshold is dependent on modulation amplitude (Kelly, 1961). Pokorny et al (1989) used the amplitude template to fit data collected at a frequency of 15 Hz. In our experiment, the average illuminance of the standard primary 561 nm was kept constant, but the average illuminance of the test light was varied. The frequency of the square-wave temporal modulation was 6 Hz. The results of fitting were compared with both templates.

HMP results for center primaries are shown in Figure 3. The equiluminant points obtained with the 2 templates differed by 0.02 to 0.08 log unit. For both observers, the contrast template fits were accepted because the root mean square residuals for the fits were lower than for the amplitude template for most of the data sets. For both observers, the prereceptoral filter corrections from center and surround HMP agreed within 5%. At 459 nm, the prereceptoral filtering for observer H.S. was 20% higher (.079 log unit) than that for observer S.S.

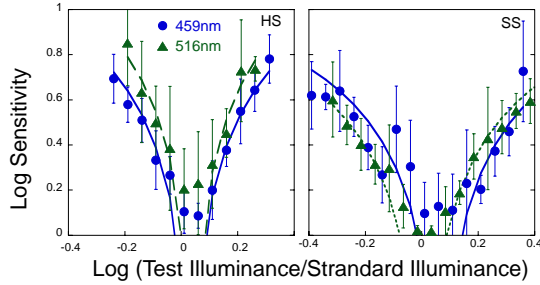


Figure 3. Heterochromatic modulation photometry (HMP) results of center primaries for 2 observers. The left panel shows data for observer H.S., and the right panel shows data for observer S.S. The circles represent HMP for 561 and 459 nm, and the triangles represent HMP for 561 and 516 nm. The lines represent the contrast template fits.

### Colorimetric Match

The observer was asked to make a successive color match between the mixture of center (or surround) 459 + 561 nm and the mixture of center (or surround) 516 + 664 nm at about 390 photopic td. The 459-, 516-, and 561-nm primaries were fixed at the expected match values calculated from the standard observer with correction for individual prereceptoral filtering determined by HMP. Only the radiance of 664 nm was adjustable. The observer pressed a button to switch between the 2 epochs, and adjusted the amount of 664 nm until a satisfactory color match was made (ie, the observer could not identify the direction of color difference between the 2 center epochs). The difference in 664-nm settings between the individual and the standard observer was used to correct for prereceptoral filter variation at 664 nm.

Both observers could make satisfactory color matches: When center 459 + 561 nm was matched to center 516 + 664 nm, the observers could not tell the direction of the chromatic difference between the 2 stimuli. Therefore, the 2 observers, though differing slightly in prereceptoral filtering, both had receptor spectral sensitivities at the colorimeter primaries that could be approximated by linear transforms of CIE 10° standard observer data.

To transform from the CIE 10° color matching into cone-based chromaticity, we used the Smith-Pokorny transformation (Smith & Pokorny, 1975) applied to the 1964 10° color-matching functions (Shapiro et al):

$$\begin{bmatrix} \bar{l}_{10}(\lambda) \\ \bar{m}_{10}(\lambda) \\ \bar{s}_{10}(\lambda) \end{bmatrix} = \begin{bmatrix} +0.15516 & +0.54308 & -0.03287 \\ -0.15516 & +0.45692 & +0.03287 \\ 0.00000 & 0.00000 & +1.00000 \end{bmatrix} \begin{bmatrix} \bar{x}_{10}(\lambda) \\ \bar{y}_{10}(\lambda) \\ \bar{z}_{10}(\lambda) \end{bmatrix} \quad (7)$$

### Rod Induction

The nulling technique that we used is similar to that employed by Krauskopf et al (1986) and Zaidi et al (1991). Figure 4 shows a schematic diagram of the method. When an observer perceives an annular surround change from bright to dark, a center field of the time-average luminance of the surround will appear to change from dark to bright. By adding luminance modulation to the center, the induced brightness change can be nulled, and the center may appear steady again. In our experiments, the rod activity in an annular surround was modulated. If there was a perceptual change in the center, the observer attempted to null or minimize the change by adding modulation to the center.

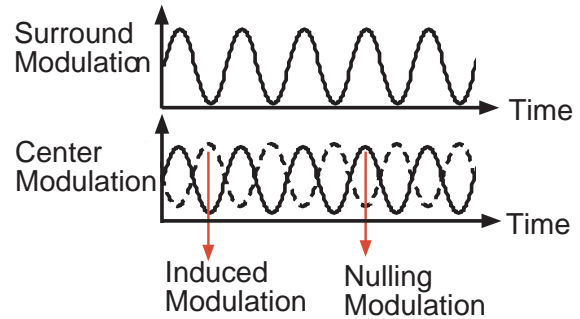


Figure 4. Schematic diagram of the nulling method. The surround is temporally modulated. The induced modulation (dashed line) in the center is nulled by the nulling modulation (solid line).

The surround-inducing modulation was a rod-temporal modulation. The center-nulling modulation was either rod or cone (S+M+L) modulation. For the (S+M+L) cone nulling, the nulling modulation amplitudes of all 3 cone types were varied together, maintaining a constant chromaticity. We ran 3 additional conditions. (1) In one condition, we varied the phase offset between the surround (inducing) and center (nulling) modulations by fixing the surround at the maximal inducing contrast and the center at the best nulling contrast measured without phase offset. The observer adjusted the phase offset between center and surround modulation to obtain minimal perceptual modulation of the center. (2) Because the observers noted a small change in hue at the best cone- (S+M+L) nulling modulation, we evaluated whether variation in chromaticity could reduce the residual center modulation. The observer could vary the magnitude of S-cone modulation ( $k_S$ ), with the M- and L-cone modulations fixed at the same contrast as the best (S+M+L) cone-nulling contrast. In this procedure,

variation in  $k$  altered the chromaticity of the modulated component of the nulling stimulus. (3) We also ran a condition in which the surround-inducing modulation was a cone-temporal modulation. We used a rod-nulling modulation of the central test field to cancel the induced cone modulation.

The temporal profile of the modulation was either square-wave, an on-pulse train, or an off-pulse train (Figure 5). The modulation frequency was 1 Hz. The time-average chromaticity of both center and surround was metameric to the equal energy spectrum ( $s = 1, l = 0.67$ ). For the square-wave condition, the time-average illuminance of center and surround was the same, either 0.1, 1, 10, or 100 photopic td (0.052, 0.52, 4.83, 48.26 scotopic td). The scotopic values do not scale exactly the photopic values because the time-average scotopic troland was varied to get maximum rod contrast at 0.1 and 1 td. For the on-pulse or off-pulse condition, the minimum or maximum center or surround illuminance was fixed at the average illuminance levels of the square-wave condition, and time-average illuminance changed with modulation contrast.

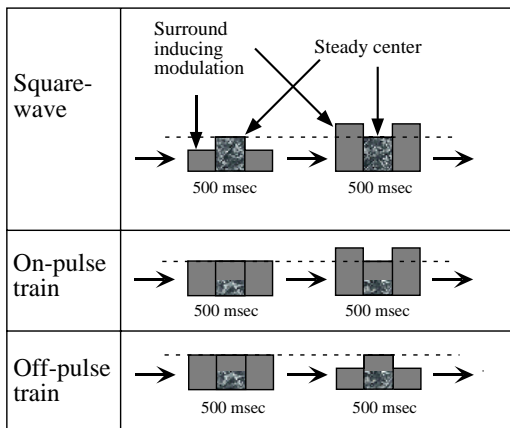


Figure 5. Temporal configurations of the stimuli for induction. There were 3 temporal profiles: square-wave, on-pulse train, and off-pulse train. In the square-wave condition, the surround was modulated around the steady center illuminance level. In the on-pulse condition, the surround had only incremental changes. In off-pulse condition, the surround had only decremental changes.

In each experimental session, the type of photoreceptors modulated in the center and surround was fixed, and there were 7 to 8 inducing contrasts with 5 settings at each. The inducing contrasts were randomized from trial to trial. The nulling contrasts and standard deviations were based on 10 settings.

## Results

Rod modulation caused induction at all 4 light levels, from 0.1 to 100 photopic td. At 10 td and 100 td, the perceptual change in the center induced by surround-rod modulation could not be effectively nulled by either rod or cone modulation. The same result occurred with a sine-wave modulated rod-inducing stimulus. At 1 td, the perceptual change of the center caused by surround-rod modulation could be nulled by either rod or (S+M+L) cone modulation, although the nulling with (S+M+L) cone modulation was not perfect. With the amplitude of the nulling stimulus fixed at its best contrast, we tried varying the relative phase of the rod-inducing and cone-nulling stimuli, but this did not eliminate the residual perceptual modulation. At 0.1 td, the center perceptual change induced by surround-rod modulation could be nulled only by rod modulation; this retinal illuminance was below cone threshold.

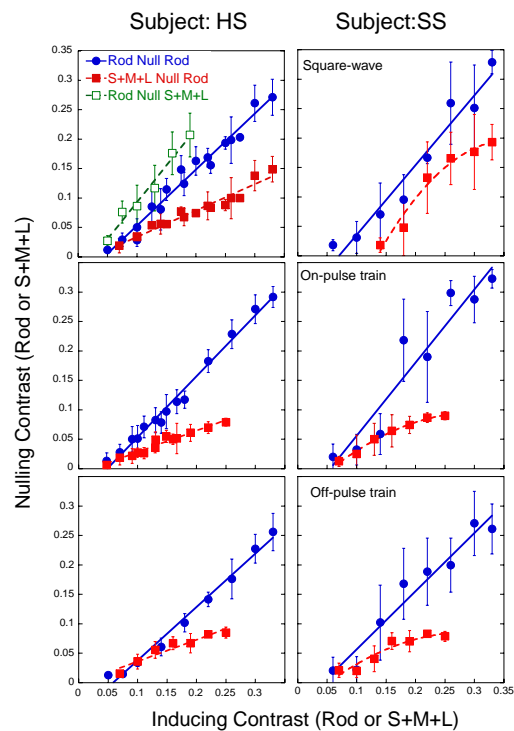


Figure 6. Rod induction with rod or cone nulling and cone induction with rod nulling at 1 td. The left panels show data for observer H.S., and the right panels show data for observer S.S. Upper panels show square-wave modulation data, middle panels show on-pulse modulation data, and lower panels show off-pulse modulation data. Circles represent rod induction with rod nulling data, solid squares represent rod induction with cone nulling data, and open squares represent cone induction with rod nulling data. The solid and dashed lines represent linear or polynomial fits.

Table 1. Fitting equations for the induction conditions

Inducing	Nulling	Retinal Illuminance (td)	Temporal Profile	Fitting Equations	
				Observer H.S.	Observer S.S.
Rod	Rod	1	Square	$y=-0.04+0.95x$	$y=-0.08+1.19x$
			On-pulse	$y=-0.05+1.04x$	$y=-0.07+1.24x$
			Off-pulse	$y=-0.05+0.91x$	$y=-0.04+0.99x$
	S+M+L	1	Square	$y=-0.01+0.445x$	$y=-0.31+2.82x-3.94x^2$
			On-pulse	$y=-0.008+0.36x$	$y=-0.05+0.95x-1.55x^2$
			Off-pulse	$y=-0.001+0.37x$	$y=-0.04+0.88x-1.53x^2$
	Rod	0.1	Square	$y=-0.05+0.89x$	$y=-0.12+1.56x$
			On-pulse	$y=-0.05+0.98x$	$y=-0.03+1.14x$
			Off-pulse	$y=-0.05+0.93x$	$y=-0.08+1.22x$
	kS+M+L	1	Square	$y=-0.12+1.41x$	$y=-0.20+1.66x$
S+M+L	Rod	1	Square	$y=-0.031+1.25x$	

All fits except one have an  $R$  value between 0.95 and 0.99.

Figure 6 shows results of rod induction with rod or cone nulling, and cone induction with rod nulling at 1 td. For rod nulling of rod induction, straight lines fit the data well. The slopes of the linear fits were close to 1.0. For cone nulling of rod induction, linear fits gave good results for observer H.S., but polynomial fits gave slightly better results for observer S.S. (Table 1). The slopes of the linear fits for both observers were less than 0.5. There were no consistent differences between the results for square-wave, on-pulse, and off-pulse modulations. Rod nulling of cone induction is only shown for observer H.S. Observer S.S. reported strong residual flicker and could not find a reliable nulling contrast. The slope was about 1.25, higher than that of rod induction with rod nulling and rod induction with cone nulling.

Figure 7 shows the results of rod induction with rod nulling at 0.1 td. These data were fitted with linear functions with slope close to unity. There was little difference in rod nulling of rod induction for data obtained at 1 td and 0.1 td.

Figure 8 shows rod induction with (kS+M+L) cone nulling. For both observers, kS cone-nulling slope was about 1.5, higher than the slope of (S+M+L) cone nulling.

## Discussion

Rod modulation induced brightness contrast at all 4 light levels (0.1, 1, 10, and 100 photopic td) that we measured. For the 2 higher light levels, 10 and 100 td, the

induced-brightness changes could not be nulled by either rod or cone modulation. At 1 td, the induced percept could be nulled by either rod or cone modulation. At 0.1 td, it could be nulled by only rod modulation; this luminance level was below the cone-absolute threshold. For 1 photopic td light level, brightness change induced by cone (S+M+L) modulation in the surround could be nulled by rod modulation in the center. At this light level, the amount of rod nulling was proportional to the rod induction with a slope near 1.0, and proportional to cone (S+M+L) induction with a slope of 1.25. The amount of cone (S+M+L) nulling was about one half of the rod induction with a slope near 0.5. These slopes suggested that cone modulation was more effective than rod modulation, both as a nulling and as an inducing stimulus. We cannot determine from our data whether this is a general property of induction or whether the relative efficiencies of the rods and cones vary with relatively small variations of light level, about 1 td.

We ran the on- and off-pulse conditions to determine whether there might be parallels in induction to the anatomical (Daw, Jensen, & Bunken, 1990) and psychophysical (Russell & Wheeler, 1983) evidence of asymmetry between rod ON and OFF pathways. There was no asymmetry between incremental and decremental rod induction. This may have resulted from the range of attainable contrast for rod-isolating stimuli (up to 30%). For achromatic contrast at photopic levels, lightness and darkness induction are highly asymmetric when there are large differences between the inducer and test fields, but

roughly symmetric when the inducing luminance is close to the test luminance level (Heinemann, 1955).

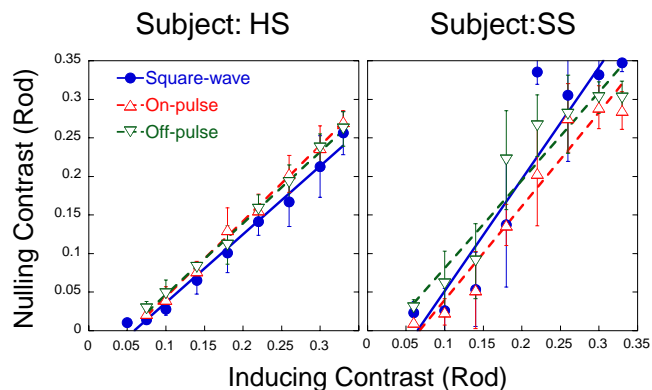


Figure 7. Rod induction with rod nulling at 0.1 td. The left panel shows data for observer H.S., and the right panel shows data for observer S.S. Circles represent square-wave data, erected-triangles represent the on-pulse data, and inverted-triangles represent the off-pulse data.

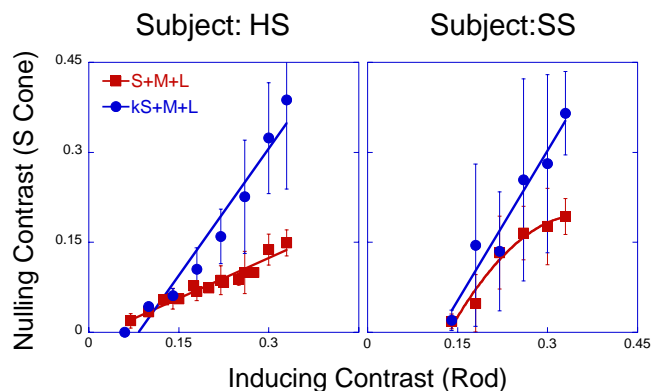


Figure 8. Rod induction with (kS+M+L) or (S+M+L) cone nulling. Squares represent (S+M+L) cone-nulling data, and circles represent (kS+M+L) cone-nulling data. For the (kS+M+L) cone-nulling condition, the center M- and L-cone contrasts were set to the nulling contrast for the (S+M+L) cone-nulling condition. For both observers, kS cone-nulling slope was about 1.5.

Both observers reported no residual flicker at the best rod nulling of rod induction, but clear residual flicker at the best cone nulling of rod induction. We tried 2 stimulus manipulations that we thought might improve the nulling. We adjusted the relative phase of the rod-inducing and cone-nulling modulations, and we varied the S-cone contribution to the cone-nulling stimulus. Phase adjustment did not improve the field appearance. Increasing the S-cone modulation to (1.5S+M+L) improved the nulling, but some residual modulation was still visible. With the assumption that the inducing and induced modulations are complementary chromaticities (Krauskopf et al, 1986; Zaidi, Yoshimi, Flanigan, &

Canova, 1992), the higher S-cone nulling stimulus may be associated with the bluish appearance of rod vision under many experimental conditions (Buck, 2001).

There are at least 2 possible reasons why we did not find a cone modulation that nulled rod induction completely. First, differing temporal responses to the rod- and cone-inducing and -nulling modulations could lead to the incomplete cancellation between the rod and cone responses. Second, rod signals are transmitted predominately in the MC pathway, according to single-unit electrophysiological studies (Gouras & Link, 1966; Lee, Pokorny, Smith, Martin, & Valberg, 1990; Lee, Smith, Pokorny, & Kremers, 1997; Purpura, Kaplan, & Shapley, 1988; Virsu & Lee, 1983; Virsu, Lee, & Creutzfeldt, 1987; Wiesel & Hubel, 1966) and psychophysical studies (D'Zmura & Lennie, 1986; Sun, Pokorny, & Smith, 2001b). Cone modulation produces responses in both the MC and PC pathways. It is possible that PC pathway cone modulation could be the source of the residual flicker.

The failure to achieve satisfactory nulls at the higher light levels may be due to a mismatch of the temporal waveforms of the induced and nulling modulations, as discussed above. Another intriguing possibility involves the lowpass temporal filter associated with induction. For both brightness and color induction, induced changes occur only at low temporal frequencies, below about 2.5 Hz (DeValois, Webster, DeValois, & Lingelbach, 1986). Magnocellular units in the primate retina and lateral geniculate nucleus show transient responses at threshold contrasts (Kaplan, Lee, & Shapley, 1990) and become more transient at high-contrast levels (Benardete, Kaplan, & Knight, 1992; Lee, Pokorny, Smith, & Kremers, 1997). If the nulling event involves the filtered sluggish temporal waveform from the inducer and the unfiltered transient waveform from the nulling stimulus, then there would be residual transient response that, if of sufficient magnitude, could produce residual flicker. The effective nulling at the lower luminance levels is consonant with reduced transience of the magnocellular responses at low luminances (Lee et al, 1990; Purpura, Tranchina, Kaplan, & Shapley, 1990). At low temporal frequencies, cone mediated function is dominated by the parvocellular system, both for achromatic (Pokorny & Smith, 1997) and chromatic stimuli. The parvocellular responses are much less transient than magnocellular responses, and parvocellular transience does not increase with contrast (Benardete et al, 1992; Lee, Pokorny, Smith, & Kremers, 1994). This may be why nulling has proven a highly effective technique in measuring photopic brightness and chromatic induction (Krauskopf et al, 1986; Zaidi et al, 1992).

## Acknowledgments

This work was supported by National Institutes of Health Grant EY00901. We thank Shuji Nakamura for furnishing the Nichia LEDs, Jules Quinlan for technical assistance in constructing the 8-channel colorimeter, Linda Glennie for programming support, and Steven Shevell and Hannah Smithson for their comments on an early draft. Publication was supported by Research to Prevent Blindness. Commercial relationships: N.

## References

- Beck, J. (1972). *Surface Color Perception*. Ithaca: Cornell University Press.
- Benardete, E. A., Kaplan, E., & Knight, B. W. (1992). Contrast gain control in the primate retina: P-cells are not X-like, some M-cells are. *Visual Neuroscience*, 8, 483-486. [PubMed]
- Buck, S. L. (1997). Influence of rod signals on hue perception: evidence from successive scotopic contrast. *Vision Research*, 37, 1295-1301. [PubMed]
- Buck, S. L. (2001). What is the hue of rod vision? *Color Research and Application*, 26, S57-S59.
- Buck, S. L., & Brandt, J. L. (1995). The range of simultaneous scotopic contrast colors. *Documenta Ophthalmologica Proceedings Series*, 58, 309-316.
- Curcio, C. A., Sloan, K. R., Kalina, R. E., & Hendrickson, A. E. (1990). Human photoreceptor topography. *Journal of Comparative Neurology*, 292, 497-523. [PubMed]
- D'Zmura, M., & Lennie, P. (1986). Shared pathways for rod and cone vision. *Vision Research*, 26, 1273-1280. [PubMed]
- Daw, N. W., Jensen, E. J., & Bunken, W. J. (1990). Rod pathways in the mammalian retinae. *Trends in Neuroscience*, 13, 110-115. [PubMed]
- DeValois, R. L., Webster, M. A., DeValois, K. K., & Lingelbach, B. (1986). Temporal properties of brightness and color induction. *Vision Research*, 26, 887-897. [PubMed]
- Gouras, P., & Link, K. (1966). Rod and cone interaction in dark-adapted monkey ganglion cells. *Journal of Physiology*, 184, 499-510. [PubMed]
- Hammond, B. R., Wooten, B. R., & Snodderly, D. M. (1997). Individual variations in the spatial profile of human macular pigment. *Journal of the Optical Society of America A*, 14, 1187-1196. [PubMed]
- Heinemann, E. G. (1955). Simultaneous brightness induction as a function of inducing- and test-field luminances. *Journal of Experimental Psychology*, 50, 89-96.
- Hendrickson, A., & Drucker, D. (1992). The development of parafoveal and mid-peripheral human retina. *Behavioural Brain Research*, 49, 21-31. [PubMed]
- Kaplan, E., Lee, B. B., & Shapley, R. M. (1990). New views of primate retinal function. In N. Osborne & J. Chader (Eds.), *Progress in Retinal Research* (Vol. 9, pp. 273-336). Oxford: Pergamon Press.
- Kelly, D. H. (1961). Visual responses to time-dependent stimuli: I. Amplitude sensitivity measurements. *Journal of the Optical Society of America*, 51, 422-429.
- Krauskopf, J. K., Zaidi, Q., & Mandler, M. B. (1986). Mechanisms of simultaneous color induction. *Journal of the Optical Society of America A*, 3, 1752-1757. [PubMed]
- Lee, B. B., Pokorny, J., Smith, V. C., & Kremers, J. (1994). Responses to pulses and sinusoids in macaque ganglion cells. *Vision Research*, 34, 3081-3096. [PubMed]
- Lee, B. B., Pokorny, J., Smith, V. C., Martin, P. R., & Valberg, A. (1990). Luminance and chromatic modulation sensitivity of macaque ganglion cells and human observers. *Journal of the Optical Society of America A*, 7, 2223-2236. [PubMed]
- Lee, B. B., Smith, V. C., Pokorny, J., & Kremers, J. (1997). Rod inputs to macaque ganglion cells. *Vision Research*, 37, 2813-2828. [PubMed]
- Moreland, J. D., & Bhatt, P. (1984). Retinal distribution of macular pigment. *Documenta Ophthalmologica Proceedings Series*, 39, 127-132.
- Pokorny, J., & Smith, V. C. (1997). Psychophysical signatures associated with magnocellular and parvocellular pathway contrast gain. *Journal of the Optical Society of America A*, 14, 2477-2486. [PubMed]
- Pokorny, J., Smith, V. C., & Lutze, M. (1989). Heterochromatic modulation photometry. *Journal of the Optical Society of America A*, 6, 1618-1623. [PubMed]
- Purpura, K., Kaplan, E., & Shapley, R. M. (1988). Background light and the contrast gain of primate P and M retinal ganglion cells. *Proceedings of the National Academy of Sciences, USA*, 85, 4534-4537. [PubMed]

- Purpura, K., Tranchina, D., Kaplan, E., & Shapley, R. M. (1990). Light adaptation in the primate retina: Analysis of changes in gain and dynamics of monkey retinal ganglion cells. *Visual Neuroscience*, *4*, 75-93. [PubMed]
- Russell, P. W., & Wheeler, T. G. (1983). Scotopic sensitivity to ON and OFF stimulus transients. *Vision Research*, *23*, 525-528. [PubMed]
- Shapiro, A. G., Pokorny, J., & Smith, V. C. (1996). Cone-rod receptor spaces, with illustrations that use CRT phosphor and light-emitting-diode spectra. *Journal of the Optical Society of America A*, *13*, 2319-2328. [PubMed]
- Smith, V. C., & Pokorny, J. (1975). Spectral sensitivity of the foveal cone photopigments between 400 and 500 nm. *Vision Research*, *15*, 161-171. [PubMed]
- Stabell, U., & Stabell, B. (1975). Scotopic contrast hues triggered by rod activity. *Vision Research*, *15*, 1119-1123. [PubMed]
- Stabell, U., & Stabell, B. (1978). Scotopic hues of simultaneous contrast. *Vision Research*, *18*, 1491-1496. [PubMed]
- Sun, H., Pokorny, J., & Smith, V. C. (2001a). Control of the modulation of human photoreceptors. *Color Research and Application*, *26*, S69-S75.
- Sun, H., Pokorny, J., & Smith, V. C. (2001b). Rod-cone interactions assessed in inferred magnocellular and parvocellular postreceptoral pathways. *Journal of Vision*. In Press.
- Sung, C. H., Davenport, C. M., Hennessey, J. C., Maumenee, I. H., Jacobson, S. G., Heckenlively, J. R., Nowakowski, R., Fishman, G., Gouras, P., & Nathans, J. (1991). Rhodopsin mutations in autosomal dominant retinitis pigmentosa. *Proceedings of the National Academy of Sciences, USA*, *88*, 6481-6485. [PubMed]
- Swanson, W. H., Ueno, T., Smith, V. C., & Pokorny, J. (1987). Temporal modulation sensitivity and pulse detection thresholds for chromatic and luminance perturbations. *Journal of the Optical Society of America A*, *4*, 1992-2005. [PubMed]
- Virsu, V., & Lee, B. B. (1983). Light adaptation in cells of macaque lateral geniculate nucleus and its relation to human light adaptation. *Journal of Neurophysiology*, *50*, 864-878. [PubMed]
- Virsu, V., Lee, B. B., & Creutzfeldt, O. D. (1987). Mesopic spectral responses and the Purkinje shift of macaque lateral geniculate cells. *Vision Research*, *27*, 191-200. [PubMed]
- Watanabe, T., Mori, N., & Nakamura, F. (1992). A new superbright LED stimulator: Photodiode-feedback design for linearizing and stabilizing emitted light. *Vision Research*, *32*, 953-961. [PubMed]
- Wiesel, T., & Hubel, D. H. (1966). Spatial and chromatic interactions in the lateral geniculate body of the rhesus monkey. *Journal of Neurophysiology*, *29*, 1115-1156. [PubMed]
- Wyszecki, G. (1986). Color appearance. In L. K. Boff, & J. P. Thomas (Eds.), *Handbook of Perception and Human Performance* (Vol. I: *Sensory Processes and Perception*). New York: John Wiley & Sons.
- Zaidi, Q., Yoshimi, B., & Flannigan, J. (1991). Influence of shape and perimeter length on induced color contrast. *Journal of the Optical Society of America A*, *8*, 1810-1817. [PubMed]
- Zaidi, Q., Yoshimi, B., Flannigan, N., & Canova, A. (1992). Lateral interactions within color mechanisms in simultaneous induced contrast. *Vision Research*, *32*, 1695-1707. [PubMed]